Colloid Polym Sci (2008) 286:983–991
DOI 10.1007/s00396-008-1858-2

ORIGINAL CONTRIBUTION

Melting and zero growth rate temperatures of syndiotactic polystryrene

A. Sorrentino · R. Pantani · G. Titomanlio

Received: 28 November 2007 / Revised: 1 February 2008 / Accepted: 25 February 2008 / Published online: 27 March 2008

Abstract In polymer crystallization, the correct determination of the melting temperature is of crucial importance since crystallization kinetics mainly depends on the amount of undercooling. In this work, the thermodynamic melting temperature and the reference temperature for crystallization kinetics (also called "zero growth rate temperature") are calculated by means of alternative procedures with the objective of providing a general discussion on problems occurring in their determination and of identifying the relationship between them. Syndiotactic polystyrene is used as test material due to its very interesting polymorphic behavior and because many data have been recently reported in the literature concerning its melting temperature. It was found that the thermodynamic melting temperature resulting by differential scanning calorimetry heating analysis provides a poor description when applied to crystallization kinetic data. The reference temperature to be adopted in crystallization kinetic equations resulted to be significantly lower. This seems to agree with recent findings and somewhat to contradict conventional understanding.

Keywords Thermodynamic melting temperature · Crystallization kinetics · Polymer crystallization · Syndiotactic polystyrene

A. Sorrentino (✉) · R. Pantani · G. Titomanlio
Chemical and Food Engineering Department,
University of Salerno,
Via Don Melillo,
84084 Fisciano, SA, Italy
e-mail: asorrent@unisa.it

Introduction

The thermodynamic melting temperature $\left(T_m^0\right)$ represents the melting temperature of infinitely extended crystals. Crystals of linear macromolecules of large dimensions are generally difficult to obtain from direct experimental measurements; thus, it is necessary to develop extrapolation procedures to extract equilibrium data from measurements performed on metastable small crystals. These extrapolation procedures essentially imply that the crystal thickness is controlled by the undercooling below T_m^0 and that the former decreases inversely with the undercooling [1].

The most known and used of these procedures is based on the Hoffmann–Lauritzen theory (Hoffmann–Weeks [HW] procedure). Even if the HW procedure has been questioned on the basis of direct measurements of crystal thicknesses during crystallization and melting by small-angle x-ray scattering (SAXS), at the moment, it seems the only method commonly accepted in literature [2].

The reference temperature $\left(T_K^0\right)$ to be used in the kinetic description of the crystallization process in polymeric materials is also commonly referred to as melting temperature. It is perhaps the most important macroscopic quantity to characterize the crystallization kinetics of a polymer: Even small variations in the choice of T_K^0 can lead to a significant change in the magnitude of calculated crystallization kinetic parameters [1].

Strobl [2, 3], very recently, revised the existing crystallization theories, suggesting a nonperfect symmetry between melting and crystallization stages (i.e., the pathway followed during the growth of polymer crystallites differs from the one followed during melting). In other words, T_K^0 (named by Strobl et al. as "zero growth rate temperature"), based on the

growth rate experiments and theories, not necessarily coincides with the T_m^0 coming from melting experiments. The existence of T_K^0 is interpreted by Strobl as a strong indication that the HW description is not appropriate for polymer crystallization.

The objective of this work is to provide a discussion on problems occurring in the determination of the thermodynamic melting temperature (T_m^0) and its experimental relationship with T_K^0.

Syndiotactic polystyrene (sPS) was selected as the testing material due to its very interesting crystallization behavior. This material, in fact, has attracted considerable interest because of its complex polymorphic behavior and its high sensibility to processing conditions [4–11]. In particular, when crystallized from the molten state, sPS solidifies into two different crystal forms, termed α and β [5, 7].

Materials and methods

Materials

sPS (Questra QA101) was obtained as a courtesy sample material from Dow Chemical in the form of pellets. Daniel et al. [12] found for the resin of the same batch an average molecular weight (M_w) of 320 kg/mol and a content of syndiotactic triads of more than 98%.

To erase previous thermo-mechanical history and provide the same crystalline memory conditions for all the subsequent experiments, the as-received pellets were first melted in a Carver laboratory press at 300 °C, stamped into films with thickness of about 300 μm, held at this temperature for 15 min, and then cooled quickly in a bath of ice and water. X-ray characterization of the molded disks shows the typical amorphous halo, whereas infrared spectra show weak levels of absorbance in the bands (1,222, 901, and 851 cm^{-1}) due to traces of the metastable α form [13]. The sample obtained by this method was adopted for all subsequent treatments and will be referred to as the "starting sample."

Calorimetric experiments

An important factor in determining overall crystallization kinetics and final morphology of sPS is the crystalline memory of the α phase, which is maintained in a wide temperature range above the melting temperature [8–11]. These memory effects allow the control of the final morphology of the sPS samples, such that information about the properties of a single phase can be obtained [11].

The crystallization behavior of sPS was investigated using a differential thermal analyzer (DTA) "Mettler DSC 822" in flowing nitrogen atmosphere. To ensure reliability of the data obtained, heat flow and temperature were calibrated with standard materials, indium and zinc, both before and after the experiments. With the aim of minimizing the thermal lag between the polymer sample and the DTA sensor, the sample cups were always loaded with flat samples weighing about 5 mg. Starting samples were heated up to T_{ann} (290 and 345 °C) with the same heating rate of 100 °C/min. After selected annealing protocols (either 1 min at 290 °C or 15 min at 345 °C, chosen as to either preserve and or erase the memory of the previous crystallization), the samples were cooled to the test temperature (T_c) at a rate of 100 °C/min [11]. To verify the absence of any degradation (especially for the highest applied annealing temperatures), some experiments were repeated twice on the same sample. The reproducibility of results was assumed as a proof that no degradation occurred in our samples.

Both annealing protocols were chosen on the basis of our previous results [11]: All the samples annealed at 290 °C crystallized into the α phase, whereas samples annealed at 345 °C crystallized into the β form.

In agreement with Hoffman–Weeks assumptions, the time spent at T_c was chosen to reach a low crystallinity level where the thickening effect of lamellae, if any, is greatly limited [1]. To this goal, at each crystallization temperature, the described thermal cycle was performed with at least two different crystallization times. In the first cycle, the time spent at T_c was chosen longer than the time needed to complete the exothermic differential scanning calorimetry (DSC) peak. The second run was stopped at a time such to reach about 5% of the enthalpic peak of the first run. The temperature was then raised up to complete fusion, and the peak temperature of the melting endotherm was taken as the melting point.

Concerning the procedure, an important factor to take into account is the heating rate employed during the melting stage. A low heating rate can allow reorganization, whereas a high heating rate can induce strongly superheating in the polymer samples [14]. For these reasons, the peak maximum temperature should be determined by an optimum heating rate scanning, even though an error is always present with the best conditions.

To measure the melting point of the original crystals, high heating rates are needed; however, the thermal lag of a DSC cell causes a shift of the melting peak to a higher temperature. From the theory of a heat-flow calorimeter, it follows that this error is proportional to the square root of heating rate, heat of fusion, and sample mass. The melting point of the crystals present in a polymer sample should be measured using different high heating rates and constant sample mass. Assuming that the melting temperature does not depend on heating rate, a good approximation of the

melting point can be found by plotting the melting peak temperatures as a function of the square root of the heating rate. Thus, all melting peak temperatures were recorded at constant samples weight but with different heating rates (ranging between 5 and 20 °C/min) and extrapolated to a zero heating rate ("corrected melting temperature").

Experimental results

The equilibrium melting temperature

The melting traces of sPS crystallized at different temperatures from the melt show a complex behavior [15, 16]. In agreement to the previous literature results [15–18], the majority of thermal heating traces obtained in this work exhibited two or three major endothermic peaks. Figures 1 and 2 illustrate plots of the temperature of the peaks as a function of the crystallization temperature (T_c) and annealing procedures.

In both series of samples, the highest melting temperature is essentially independent on the crystallization temperature. It was generally associated with the crystals that reorganize during the heating scan. The samples crystallized in the β phase morphology (annealed at 345 °C) show a minor melting peak just above T_c. It was ascribed [16, 17] to annealing effect on the less perfect β crystals formed at low temperatures. As suggested in previous literature results, the melting peak of the original crystals present in the samples was thus associated to the lowest and the intermediate melting peak temperatures for the α and β phases, respectively.

A linear extrapolation was conducted on the corrected melting peak (corrections were made following the procedure indicated in the section above) according to the classical Hoffman–Weeks equation:

$$T_m = T_m^0\left(1-\frac{1}{\gamma}\right)+T_c\frac{1}{\gamma} \quad (1)$$

in which γ is the lamellar thickening coefficient. This method of estimating T_m^0, although quite often adopted, is incorrect on a rigorous ground due to several assumptions made on the overall lamellar thickness [19]. The results of the method are shown in Figs. 1 and 2 (dotted lines).

From such a linear extrapolation, the equilibrium melting temperature of the α form is determined as 272 °C, whereas the equilibrium melting temperature of the β form is determined as 282 °C (Table 1). These results are compared in Figs. 3 and 4 (for α and β phase, respectively) with literature results.

Ho et al. [20] using the same procedure as discussed here for preparing samples in neat α and β forms found for a resin with M_w=67 kg/mol equilibrium melting temperatures equal to 272 and 278.6 °C for α and β crystals form,

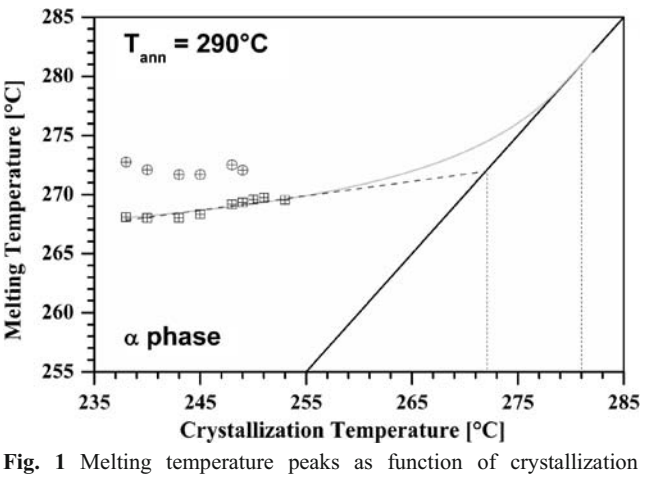

Fig. 1 Melting temperature peaks as function of crystallization temperature for samples annealed at 290 °C. *Dashed line*: linear HW extrapolation ($T_m^0 = 272.1\ ^\circ C$); *continuous line*: nonlinear HW extrapolation ($T_m^0 = 281\ ^\circ C$)

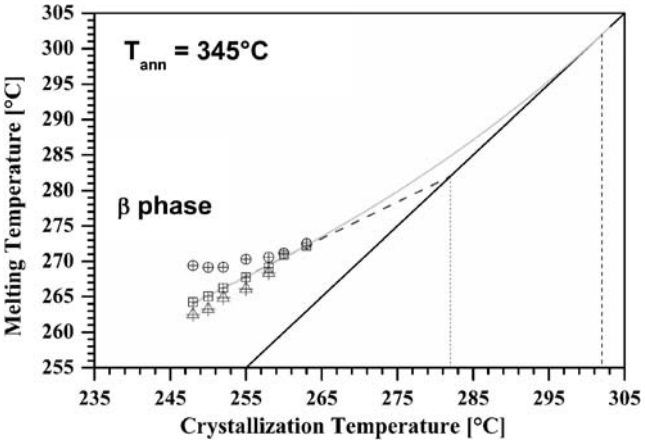

Fig. 2 Melting temperature peaks as function of crystallization temperature for samples annealed at 345 °C. *Dashed line*: linear HW extrapolation ($T_m^0 = 282\ ^\circ C$); *continuous line*: nonlinear HW extrapolation ($T_m^0 = 302\ ^\circ C$)

Table 1 Melting temperatures of sPS, as calculated by different authors and adopting different extrapolation procedures

Temperature	Method	Values	Reference
$T_{m\alpha}^0$; $T_{m\beta}^0$	Linear extrapolation	272; 282 °C	This work
$T_{m\alpha}^0$; $T_{m\beta}^0$	Linear extrapolation	272; 278.6 °C	[20]
$T_{m\alpha}^0$; $T_{m\beta}^0$	Linear extrapolation	281.3; 291 °C	[15]
$T_{m\alpha}^0$; $T_{m\beta}^0$	Nonlinear extrapolation	294; 320 °C	[15]
$T_{m\alpha}^0$; $T_{m\beta}^0$	Nonlinear extrapolation	282; 295 °C	This work
$T_{m\alpha}^0$; $T_{m\beta}^0$	Nonlinear extrapolation	281; 288 °C	[22]
$T_{m\alpha}^0$; $T_{m\beta}^0$	Kinetic data	272; 283 °C	This work
$T_{m\alpha}^0$; $T_{m\beta}^0$	Gibbs–Thomson plot	282; 292 °C	This work
$T_{m\alpha}^0$; $T_{m\beta}^0$	Gibbs–Thomson plot	281; 292.7 °C	[26, 27]

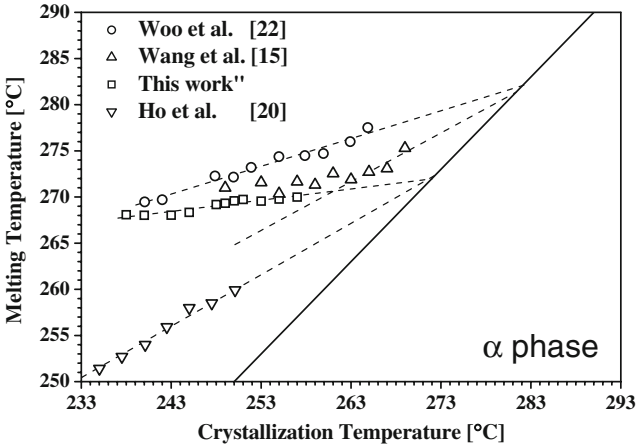

Fig. 3 Linear HW extrapolation for melting temperature as a function of crystallization temperature in sPS annealed at 290 °C

respectively (Figs. 3 and 4). The differences between these values and our results are very small and can be probably attributed to both experimental uncertainties and to the difference in the resins adopted (Table 1).

Wang et al. [15] (M_w=200 kg/mol) using a press-molding procedure for preparing the specimens reported the equilibrium melting temperatures equal to 281.3 and 291 °C for α and β forms, respectively. In addition, they found that in their case, the assumptions on which are based the linear HW plot is not completely verified. In their case, in fact, the relation between the intermediate melting peak and the crystallization temperature exhibits a slight curvature, so that, for the α phase (Fig. 3), they considered for the linear extrapolation only the points collected at the highest temperatures.

Wang et al. [15] carried out a nonlinear extrapolation based on Marand's method [19, 21] obtaining a value of 294 and 320 °C for the α and β forms, respectively (Table 1).

The Marand's method was also applied to our data as shown in Figs. 1 and 2 (as continuous lines). The resulting values for the equilibrium melting temperatures are 282 and 295 °C for the α and β forms, respectively.

Woo et al. [22], adopting the nonlinear HW relation, found the T_m^0 of α and β crystals to be 281 and 288 °C, respectively. Unfortunately, the authors do not report any additional information on the experimental procedure applied.

It is important to point out that precautionary remarks regarding the use of the nonlinear method were addressed in detail in the original publication by Marand et al. [19]. In particular, the authors [19] suggest that scatter in the data and slight variations in γ with temperature can prevent the correct determination of the melting temperature.

However, it is interesting to notice that for β phase, our experimental results are very close to the results obtained by Wang et al. [15] and also to those reported by Woo et al. [22]. In spite of this, the results obtained for T_m^0 are quite different (see Table 1). These differences are mainly due to the different range of temperature investigated.

Our experimental range was limited by two factors: for the α phase samples, at low temperature, the achievable cooling rate (100 °C/min) does not allow to reach lower isothermal crystallization temperature (smaller than 238 °C) before the crystallization starts. On the other side, at a higher temperature (greater than 252 °C), despite the annealing temperature, the formation of β crystals cannot be excluded. For the β phase samples, low temperatures (smaller than 248 °C) are prohibited due to the formation of α crystals. The data of Wang et al. [15] and Woo et al. [22] cover a larger crystallization temperature range probably because they used a special method for sample preparation. Atypical preparation methods, however, can increase the risk involved in extrapolating to temperatures well above T_m for the presence of a sensible amount of the mesomorphic phase and/or frozen-in stresses.

In agreement with all literature results [15, 20, 22] and despite the extrapolation methods adopted, the thermodynamic equilibrium melting temperature T_m^0 of the β crystalline form in sPS was found to be higher than that of the α form. On the basis of thermodynamic equilibrium, the higher value of T_m^0 in the β form may be attributed to the lower value on the entropy of fusion and/or the higher value on heat of fusion (Fig. 2). The orthorhombic chain packing of β form crystals is more stable than the trigonal chain packing of α form crystals. However, the experimental melting temperature of a single α form is higher than the melting temperature of a single β form at low crystallization temperatures (Figs. 1 and 2). This result suggests that the behaviors of sPS polymorphism exhibit a phenomenon of phase stability inversion with lamellar size [20, 22].

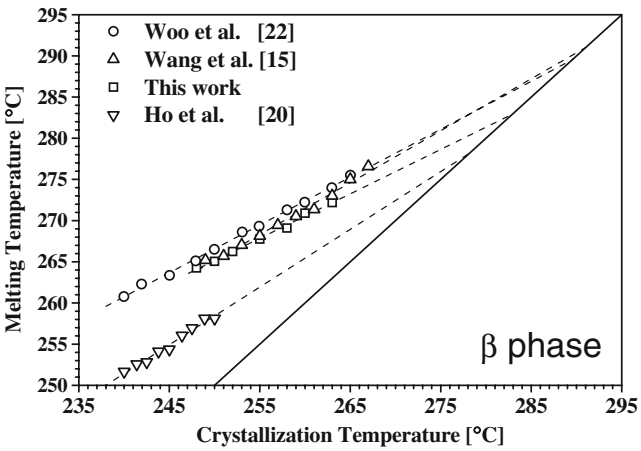

Fig. 4 Linear HW extrapolation for melting temperature as a function of crystallization temperature in sPS annealed at 345 °C

Isothermal crystallization

In our previous work [11], isothermal melt and cold crystallization tests were carried out. Isothermal melt crystallization tests were performed by cooling the starting samples, molten at two temperatures (290 and 345 °C), rapidly to the crystallization temperature. Samples annealed at 290 °C show a higher crystallization rate [11]. From the curves shown in Figs. 8 and 9 of our previous work [11], the half-time of crystallization $t_{1/2}$, defined as the time required for half of the final crystallinity to develop, was obtained.

Isothermal cold crystallization tests were performed by heating the starting samples rapidly to T_c. These samples only showed crystals in the α phase. The open diamonds in Fig. 5 refer to the half-time of crystallization of these second kinds of samples [11].

According to the Lauritzen–Hoffman theory [1], the crystallization growth rate can be written as:

$$G(T) = G_0 \exp\left[-\frac{U}{R(T-T_\infty)}\right] \exp\left[-\frac{K_g\left(T_K^0+T\right)}{2T^2(T_K^0-T)}\right] \quad (2)$$

where G_0 is the growth rate factor (μm/s), the first exponential term (Vogel–Fulcher–Tamman–Hesse equation [VFTH]) contains the contribution of the diffusion process to the crystallization rate, whereas the second exponential term is the contribution of the nucleation process.

$G(T)$ is implicitly contained in the overall crystallization rate constant $K(T)$ experimentally determined by the half crystallization time ($t_{1/2}$). The temperature dependence of K is often written as:

$$K^{1/n}(T) = k_0 \exp\left[-\frac{U_t}{R(T-T_\infty)}\right] \exp\left[-\frac{K_t\left(T_K^0+T\right)}{2T^2(T_K^0-T)}\right] \quad (3)$$

In this case, K_t takes into account simultaneously nucleation and growth processes, and n is the Avrami index. According to the original derivation of Eq. 2, the reference temperature T_K^0 coincides with the equilibrium melting temperature T_m^0. Equations 2 and 3 are widely used but, in spite of their derivation that would impose to adopt T_m^0 instead of T_K^0, have proven to well describe the temperature dependence of growth rate and crystallization kinetics data for many polymer systems by letting T_K^0 be different from T_m^0 [23].

The universal values proposed for the VFTH parameters in Eq. 2 for the growth rate description are U=1,500 cal/mol and $T_\infty = T_g - 30\,^\circ C$, T_g being the glass transition temperature (T_g=100 °C for sPS) in contrast to the values U=4,120 cal/mol and $T_\infty = T_g - 51.6\,^\circ C$ coming from the rheological measurements. However, it can be easily understood that the uncertainties in U and T_∞ values lead to a negligible effect on the crystal growth rate when, as for sPS, crystallization takes place far above T_g.

A multivariable regression software was adopted to obtain the best fitting parameters of Eq. 3 targeting the experimental data of Fig. 5. Assuming for U_t and T_g the universal values (common to both phases), the unknown parameters are K_t, k_0, and T_K^0 (for α and β phase).

With the values adopted for U_t and T_g, Eq. 3 was not able to fit simultaneously experimental data at high and low temperatures for the α phase, irrespective of the values given to K_t and k_0. Therefore, the cold crystallization data were excluded from the target, and the continuous lines in Fig. 5 represent the best fitting to the melt crystallization data assuming the universal values for the VFTH parameters. The parameters found are listed in Table 2 column headed "Melt crystallization."

As a further step, the parameters of the VFTH equation were left free. As shown by the dotted line in Fig. 5, in this case, the model is able to describe correctly all set of experimental data. The parameters are reported in Table 2, with the column headed "Full-range crystallization."

The activation energy tuned on cold crystallized data is sensibly lower than the universal value for the melt crystallized sample, inducing weaker temperature dependence. Such differences in activation energy are consistent with data reported by Lu and Nutt [24].

As reported in Fig. 5, a curve of $K(T)$ can be drawn with a minimal degree of error over the whole temperature range (i.e., $T_g \le T_c \le T_K^0$).

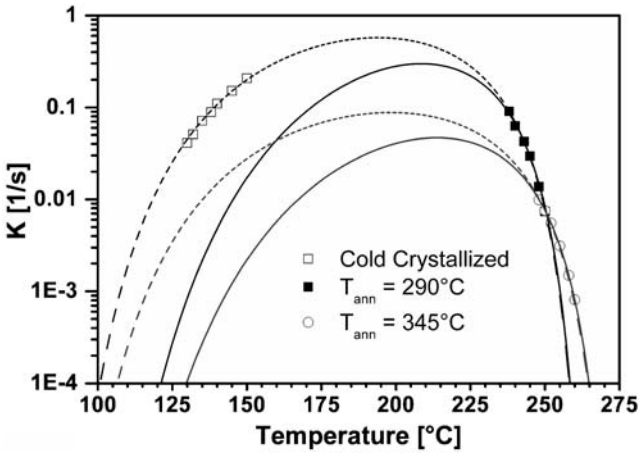

Fig. 5 Crystallization rate constant for versus temperature for specimens annealed at 290 and 345 °C, respectively. *Continuous line* are obtained with U_t=1500 cal/mol in Eq. 3, while *dotted line* is obtained by simultaneous fitting of data from samples melt and cold crystallized in the α form (obtaining U_t=775 cal/mol in Eq. 3)

Table 2 Parameters found for our resin

Parameters	Melt crystallization	Full-range crystallization	Growth rate
k_0–G_0	$k_{0\alpha}$=1,603/s	$k_{0\alpha}$=194/s	$G_{0\alpha}$=677 μm/s
k_0–G_0	$k_{0\beta}$=222/s	$k_{0\beta}$=29/s	$G_{0\beta}$ =1,083 m/s
U	$U_{t\alpha}$=1,500 cal/mol	$U_{t\alpha}$=775 cal/mol	U_{α}=1,500 cal/mol
U	$U_{t\beta}$=1,500 cal/mol	$U_{t\beta}$=775 cal/mol	U_{β}=1,500 cal/mol
K	$K_{t\alpha}$=89,800 K^2	$K_{t\alpha}$=89,800 K^2	$K_{g\alpha}$=45,800 K^2
K	$K_{t\beta}$=100,000 K^2	$K_{t\beta}$=100,000 K^2	$K_{g\beta}$=88,000 K^2
n_α	1.5	1.5	
n_β	3.5	3.5	
$T^0_{K\alpha}$ [K]	(272+273.15)	(272+273.15)	(272+273.15)
$T^0_{K\beta}$ [K]	(283+273.15)	(283+273.15)	(283+273.15)
T_g [K]	(100+273.15)	(100+273.15)	(100+273.15)

A sensitivity analysis was performed by imposing the value of T^0_K and letting the regression routine find the values of k_0 and K_t. The differences between predicted values and experimental data were recorded in terms of variance. As show in Fig. 6, the minimum in the variance was obtained for the two sets of data (U_t=1,500 cal/mol and U_t=775 cal/mol) for values of T^0_K falling in a very narrow range (less than 3 °C). This confirms that the value chosen for U_t induces small changes in the T^0_K values determined from least-squares fitting analysis. On the contrary, the parameter K_t was found to be very sensitive to the value of T^0_K. For example, an increase of 10 °C in the assigned melting temperature resulted in an increase of about one order of magnitude for K_t.

The results of the regression procedure provide for T^0_K the values of 272 and 283 °C for the α and β phases, respectively. These values are in very good agreement with the values found by the linear HW extrapolation and sensibly lower than those obtained by the nonlinear extrapolation (see Table 1).

Literature growth rate data

To prove the reliability of the values found for T^0_K, they were employed to describe some growth rate data present in literature. Experimental data of spherulitic growth rates for the α phase of sPS measured at temperatures between 235 and 252 °C, taken from Chiu et al. [10] are plotted, as a function of the crystallization temperature, in Fig. 7. Furthermore, experimental data of spherulitic growth rates of sPS cold crystallized isothermally at various temperatures ranging between 115 and 150 °C, taken from Wang et al. [25], are there reported. Experimental data of spherulitic growth rates for the β phase measured at temperatures between 251 and 265 °C were taken from Wang et al. [25] and are also shown in Fig. 7.

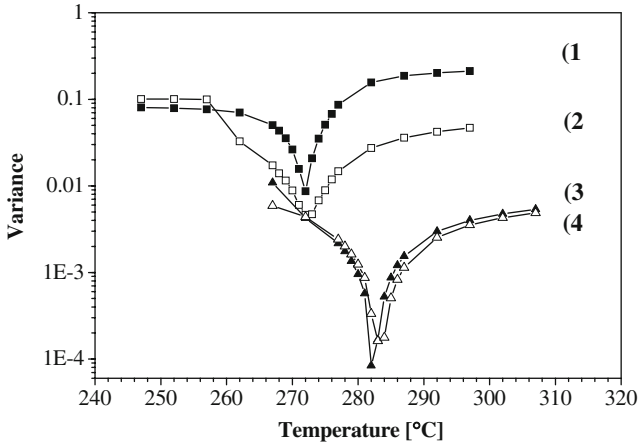

Fig. 6 Results of the least-square fitting as a function of equilibrium melting temperature, T^0_K for: *1* full set of data (melt and cold crystallization) of samples crystallized in the α form; *2* data from melt crystallization of samples crystallized in the α form; *3* data from melt crystallization of samples crystallized in the β form; *4* full set of data (melt and cold crystallization) of samples crystallized in the β form

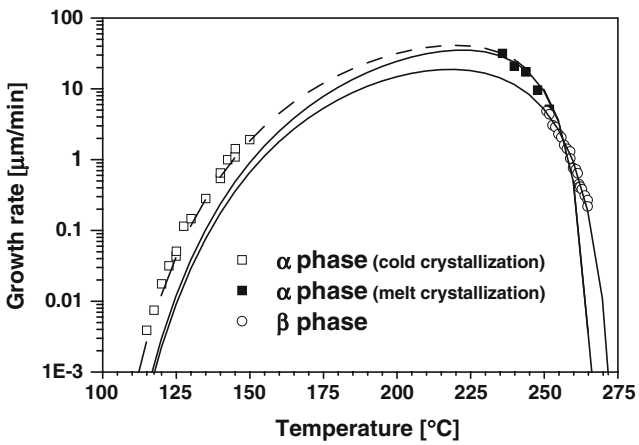

Fig. 7 Growth rate data of the α and β forms at different crystallization temperatures (*open diamonds* are obtained from [25], *filled diamonds* are obtained from [10], *filled circles* are taken from [26]). *Lines* are the results of Eq. 2 with parameters reported in Table 1. The *dashed line* is obtained using U=1,360 cal/mol and $G_{0\alpha}$=420 μm/s in Eq. 2

Table 3 Parameters used in equations 4 and 5

Parameters	Growth rate Data	Reference
a [nm]	0.441	[27]
b [nm]	0.72	[27]
ρ_α [g/cm^3]	1.033	[7]
ρ_β [g/cm^3]	1.066	[7]
Δh_α [J/g]	49.7	[11]
Δh_β [J/g]	56.7	[11]
$K_{t\alpha}$ [K^2]	45800	This work
$K_{t\beta}$ [K^2]	88000	This work
$T^0_{K\alpha}$[K]	(272+273.15)	This work
$T^0_{K\beta}$[K]	(283+273.15)	This work

A regression procedure was adopted to find the parameters of Eq. 2 for the best description of the data reported in Fig. 7.

In particular, to describe the experimental data of the growth rate, only the parameters G_0 and K_g were best fitted, T^0_K and T_g were left unchanged, and U was taken as the universal value of 1,500 cal/mol.

The calculated growth rates (according to Eq. 2 adopting the set of parameters listed in Table 1 "Growth rate" column were adopted) are reported in Fig. 7 as continuous lines. It is evident that the set of parameters found well describes the literature growth rate data, over the entire range. The minor deviation from the data at a lower temperature for the α phase is probably due to the VFTH universal values used for the parameters. As shown in Fig. 7, a better description was obtained using different values for U and $G_{o\alpha}$ namely, U=1,360 cal/mol and $G_{o\alpha}$=420 μm/s.

Discussion of results

The nucleation parameter appearing in the growth rate Eq. 2, K_g, depends on the growth regime [1] and is given by:

$$K_g = \frac{4b\sigma_{ec}\sigma_{en}T^0_K}{B\Delta h k_b} \quad (4)$$

where b is the thickness of a monomolecular layer, σ_{en} and σ_{ec} are the lateral and the fold surface free energy, respectively, k_b is the Boltzmann constant, and B is a constant equal to 1 at high and at low crystallization temperatures (regimes I and III, respectively) and equal to 2 in the intermediate crystallization temperature range (regime II). Δh is the bulk enthalpy of fusion per unit volume for the fully crystalline polymer.

The value of σ_{en} can be estimated by using the Thomas–Stavely equation [1]:

$$\sigma_{en} = 0.1\sqrt{ab}\Delta h \quad (5)$$

where a is the chain width and ab is the cross sectional area per chain molecule.

The K_g values as determined from the growth rate data fitting (Fig. 7 and Table 2, column headed "Growth rate") allow therefore to evaluate the values of $\sigma_{ec}/\Delta h$, from Eqs. 4 and 5 using the parameters reported in Table 3 [7, 11, 27]. In particular, the values of 0.13 and 0.22 nm were obtained for the α and β phases, respectively. The order of magnitude is the same of the values proposed by Wang et al. [26] (0.057 and 0.12 nm for α and β, respectively), and furthermore, the ratio between the two values is essentially the same.

Data of lamellar thickness, l, determined by both SAXS and transmission electron microscopy, can be found in the literature, for the α and β forms crystallized at various temperatures [26, 27].

The experimental data reported in Figs. 8 and 9 were taken from Wang et al. [25, 26]. The linear fitting reported as dotted lines in Figs. 8 and 9 was proposed by the authors according to the well-known Gibbs–Thomson relation:

$$T_m = T^0_m\left(1 - \frac{2\sigma_{ec}}{l\Delta h}\right) \quad (6)$$

The authors imposed as equilibrium melting temperature of the α and β forms the values of 281 and 292.7 °C, respectively. In addition, the extrapolation for the α phase was conducted without considering the data point at the lowest crystallization temperature (unfilled square in Fig. 8).

We tried to describe the data reported in Figs. 8 and 9 by Eq. 6, using the values of $\sigma_{ec}/\Delta h$ found in this work by describing the growth rate data.

In Figs. 8 and 9, the results of Eq. 6 in two different cases are reported. In the first case (lines 1), it is assumed

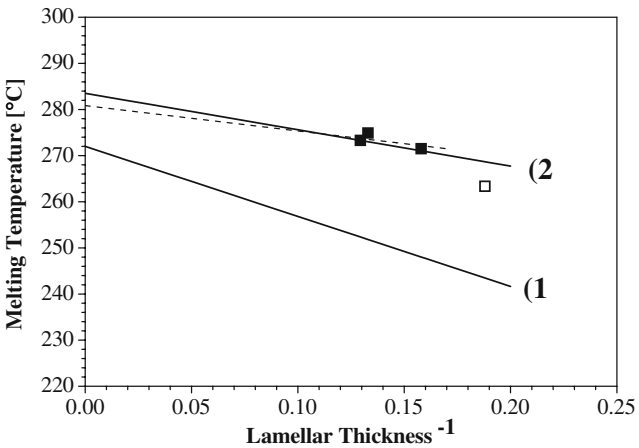

Fig. 8 Gibbs–Thomson plots of the α phase as reported by Wang et al. [28, 29]. *Dotted line* represents the linear best fitting as proposed in the literature [28, 29]; *Continuous lines* represent the linear description assuming our results for $\frac{\sigma_{ec}}{\Delta h}$ and different values for the equilibrium melting temperatures: *1* $T^0_{m\alpha} = T^0_{K\alpha}$, *2* $T^0_{m\alpha}$=282 °C, i.e., the best value to describe experimental data

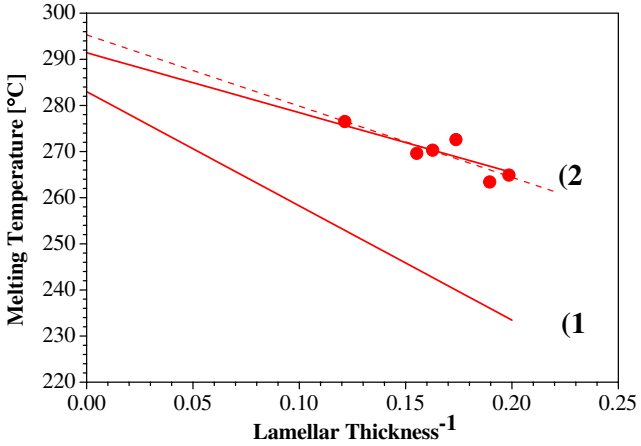

Fig. 9 Gibbs–Thomson plots of the β phase sPS as reported by Wang et al. [28, 29]. *Dotted line* represent the linear best fitting as proposed in the literature [28, 29]; *continuous lines* represent the linear description assuming our results for $\frac{\sigma_{ec}}{\Delta h}$ and different values for the equilibrium melting temperatures: *1* $T^0_{m\beta} = T^0_{K\beta}$, *2* $T^0_{m\beta}$=292 °C, i.e., the best value to describe experimental data

that $T^0_{\mathrm{m}} = T^0_K$. In this case, it is evident that the lines are well far from experimental data. However, a very good description of the experimental data can be obtained with a simple shift of the lines (that can be obtained increasing T^0_m). In other words, it is clear from these results that T^0_m cannot be assumed equal to T^0_K. It is important also to note that the T^0_m values that better describe the experimental data are 282 and 292 °C for the α and β forms, respectively. These values are closer to the nonlinear extrapolation than those obtained from the linear extrapolation (Table 1). However, it is evident that due to the very small number of data points and the large scattering between them, a univocal result from the extrapolation of data reported in Fig. 9 cannot be drawn.

In conclusion, we found both for the α and β phases two couples of melting temperatures. A first couple, $T^0_{m\alpha}$ and $T^0_{m\beta}$, was found by a nonlinear extrapolation of DSC melting peaks, adopting all the corrections needed to obtain a reliable set of data. This couple is consistent with literature data of T_{m} versus the reciprocal of lamellar thickness (l^{-1}). It has to be mentioned that despite of all the accuracy in the methods and measurements, lamellar thickening cannot be completely avoided. This means that the values found for $T^0_{m\alpha}$ and $T^0_{m\beta}$ can be somewhat overestimated with respect to the true melting temperatures. Furthermore, the literature data of T_{m} versus l^{-1} could be affected by a melting kinetics and lamellar thickening [14], thus providing observed values of T_{m} higher that the thermodynamic equation values.

A second couple, $T^0_{K\alpha}$ and $T^0_{K\beta}$, was found by a regression procedure on kinetic data, both coming from crystallization half times and growth rate measurements. This couple is sensibly lower than the first one and is consistent with a linear extrapolation procedure on DSC melting peaks.

Two possible reasons can be found for the discrepancy between the two couples:

1. The values found by the nonlinear extrapolation represent the true equilibrium melting temperature, but nevertheless the crystallization kinetics data need another reference temperature, somewhat lower. This can happen because this temperature is not strictly related to the melting of a perfect crystal but is probably affected by the metastable region just below the melting temperature. Strobl hypothesized that the formation and growth of lamellar crystallites is not a single-step process proceeding directly from the melt but follows a route over intermediate states [2]. The initial step is the creation of a mesomorphic granular solid layer, which transforms into homogeneous lamellar crystallites during the final step [2, 30, 31].
2. The temperatures T^0_m and T^0_K do coincide, but the lamellar thickening induces significant errors in the determination of the melting temperature by using data of melting, in spite of any attempt to conduct a correct experiment. The true temperature is therefore lower than what is found by a nonlinear extrapolation and closer to the value found by a linear extrapolation. In this case, the regression of kinetic data provides a good estimation of the equilibrium melting temperature.

Conclusions

The melting enthalpic traces, for each crystallinity phase of sPS, were analyzed in agreement to the linear and nonlinear HW extrapolative methods to obtain the thermodynamic equilibrium melting temperature (T^0_m). Extrapolative methods are found to be somewhat sensitive to the observed data range and perhaps to the accuracy of the experimental data obtained. However, in agreement with previous literature results and despite the extrapolation methods adopted, T^0_m of the β crystalline form in sPS was found to be higher than that of the α form.

The zero growth rate temperature (which in literature is often assumed to be equal to T^0_m) was found by analyzing data of crystallization kinetics for both phases. The same values were adopted to analyze literature data of growth rate, thus confirming the reliability of the results. Data drawn analyzing the crystallization kinetics, generally show a lower sufferance to the thickening/recrystallization process. In particular, when the temperature dependence of crystal growth rates is analyzed in the context of a crystallization kinetics theory, even small variations in the choice of T^0_K can lead to a significant change in the

magnitude of the calculated crystallization kinetic rate. This somewhat makes T_K^0 much better defined than T_m^0. However, T_K^0 value seems relatively far by the thermodynamic equilibrium melting temperature T_m^0. The discrepancy is probably related to the reliability of the kinetic model adopted to describe the experimental data.

In conclusion, the results of this work show that for sPS, the equilibrium melting temperature determined from the linear HW extrapolation may be taken only as a poor estimation of the zero growth rate temperature T_K^0.

References

1. Hoffman JD, Miller RL (1997) Polymer 38(13):3151
2. Strobl G (2006) Prog Polym Sci 31(4):398
3. Cho TY, Stille W, Strobl G (2007) Macromolecules 40(7):2596
4. Sorrentino A, Tortora M, Vittoria V (2006) New developments in syndiotactic polystyrene. In: Pandalai SG (ed) Recent research developments in applied polymer science. vol. 3. Research Signpost, India
5. Guerra G, Vitagliano V, De Rosa C, Petraccone V, Corradini P (1990) Macromolecules 23(5):1539
6. Sorrentino A, De Santis F, Titomanlio G (2007) Polymer crystallization under high cooling rate and pressure: a step towards polymer processing conditions. In: Reiter G, Strobl GR (eds) Lecture notes in physics: progress in understanding of polymer crystallization. vol. 714. Springer, Berlin, pp 329–344
7. Vittoria V (1997) Syndiotactic polystyrene. In: Olabisi O (ed) Handbook of thermoplastics. Dekker, New York
8. de Candia F, Ruvolo Filho A, Vittoria V (1991) Makromol Chem Rapid Commun 12(5):295
9. Auriemma F, Petraccone V, Dal Poggetto F, De Rosa C, Guerra G, Manfredi C, Corradini P (1993) Macromolecules 26(15):3772
10. Chiu F, Shen K, Tsai SHY, Chen C (2001) Polym Eng Sci 41 (5):881
11. Sorrentino A, Pantani R, Titomanlio G (2007) J Polym Sci B Polym Phys 45:196
12. Daniel C, Guerra G, Musto P (2002) Macromolecules 35(6):2243
13. Musto P, Tavone S, Guerra G, De Rosa C (1997) J Polym Sci B Polym Phys 35(7):1055
14. Yamada K, Hikosaka M, Toda A, Yamazaki S, Tagashira K (2003) Macromolecules 36(13):4790
15. Wang C, Hsu Y-C, Lo C-F (2001) Polymer 42:8447
16. Lin RH, Woo EM (2000) Polymer 41:121
17. Sun YS, Woo EM (2001) Macromol Chem Phys 202(9):1557
18. Sun YS, Woo EM (2000) J Polym Sci Polym Phys 38(24):3210
19. Marand H, Xu J, Srinivas S (1998) Macromolecules 31:8219
20. Ho R-M, Lin CP, Tsai HY, Woo EM (2000) Macromolecules 33:6517
21. Xu J, Srinivas S, Marand H, Agarwal P (1998) Macromolecules 31:8230
22. Woo EM, Sun YS, Yang CP (2001) Prog Polym Sci 26:945
23. van Krevelen DW (1997) Properties of polymers: their correlation with chemical structure; their numerical estimation and prediction from additive group contributions, third completely revised edition. Elsevier, Amsterdam, The Netherlands (898 pp)
24. Lu H, Nutt S (2003) J Appl Polym Sci 89:3464
25. Wang C, Lin CC, Chu CP (2005) Polymer 46:12595
26. Wang C, Liao WP, Wang ML, Lin CC (2004) Polymer 45:973
27. Chen Q, Yu Y, Na T, Zhang H, Mo Z (2002) J Appl Polym Sci 83:2528
28. Wang C, Chen CC, Hung CH, Lin KS (2004) Polymer 45:6681
29. Wang C, Cheng YW, Hsu YC, Lin TL (2002) J Polym Sci B Polym Phys 40:1626
30. Cho TY, Stille W, Strobl G (2007) Colloid Polym Sci 285(8):931
31. Strobl G, Cho TY (2007) Eur Phys J E 23(1):55